VIP Carbocations

DOI: 10.1002/anie.201007762

A Strain-Releasing Trap for Highly Reactive Electrophiles: Structural Characterization of Bowl-Shaped Arenium Carbocations**

*Alexander V. Zabula, Sarah N. Spisak, Alexander S. Filatov, Andrey Yu. Rogachev, and Marina A. Petrukhina**

Corannulene ($C_{20}H_{10}$, Scheme 1), the smallest nonplanar polyaromatic fragment of the fullerene C_{60}, has attracted a great deal of attention in the last two decades.[1] In addition to its own unique properties, corannulene serves as a primary

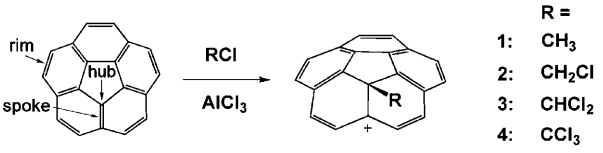

Scheme 1. Preparation of compounds (**1**–**4**)[$AlCl_4$].

model for both theoretical and experimental studies for a variety of curved carbon networks ranging from fullerenes to nanotubes. To date, the organic reactions of corannulene have been mainly limited to the derivatization of its exterior and to synthetic transformations of rim-bound functional groups.[2] Herein, we report the successful isolation of bulk crystalline products and the first X-ray crystallographic characterization of a family of nonplanar arenium carbocations $C_{20}H_{10}R^+$ (R = CH_3, CH_2Cl, $CHCl_2$, and CCl_3), obtained by electrophilic attack at the interior surface of corannulene (Scheme 1).

Corannulene reacts with halogenated hydrocarbons in the presence of $AlCl_3$ to give intense purple–blue solutions that contain $C_{20}H_{10}R^+$ cations (**1**–**4**). The formation of these cations is attributed to the abstraction of a chloride ion from the corresponding halogenated reagent followed by electrophilic attack of the in situ generated $CH_xCl_{3-x}^+$ cations at the hub C atom of $C_{20}H_{10}$. Although DFT calculations showed that the energy difference between electrophilic attacks at the hub and rim at the curved corannulene surface is small, especially when compared with the noticeably larger values for planar polyarenes,[3] only two examples of C–C bond formation at the bowl interior have been reported. Firstly, reaction of dichlorocarbene with $C_{20}H_{10}$ led to the product of the [1+2] addition to the spoke C=C bond via a zwitterionic intermediate.[4] Secondly, Scott et al. observed the formation of purple solutions as possible products of addition of transient carbocations such as $CDCl_2^+$ and CCl_3^+ to corannulene.[5] The authors ingeniously identified species formed in solution and assigned their molecular structures based on ^{1}H NMR studies of the reaction mixtures. Despite the initial progress, further elaboration proved to be unsuccessful (including recording ^{13}C NMR data), and the preparation and structural characterization of bulk solid products have not been reported to date. The latter task can be very challenging because of the extreme reactivity of the resulting cationic species.

In contrast to the behavior of corannulene, addition of $AlCl_3$ to C_{60} and C_{70} in $CHCl_3$ or $Cl_2CHCHCl_2$ provided the respective neutral products that resulted from the 1,4-addition of the above halogenated hydrocarbons.[6] Subsequent hydrolysis of these products under superacidic conditions led to the observation of the alkylated fullerene cations that had much longer lifetimes than the bowl-shaped cations, thus allowing ^{13}C NMR spectra to be recorded, although no structural studies of these species was undertaken. The solid-state structure of a fullerene cation has been elucidated from the X-ray diffraction characterization of $C_{60}(AsF_6)_2$, which was prepared in a high-pressure vessel by direct reaction of C_{60} and AsF_5 in SO_2.[7]

The arenium carbocations **1**–**4** were isolated in a pure bulk form as $[AlCl_4]^-$ salts in good (55–70%) yields. The identities of the isolated products were fully confirmed by ^{1}H and ^{13}C NMR spectroscopy, and by MALDI mass spectrometry studies.[8] Considerable time and effort were required for growing crystals of carbocations **1**–**4** that were suitable for X-ray diffraction analysis. In general, all the salts tend to solidify as nondiffracting oily materials, even when special care is given to the quality of all reagents and solvents. We found that different procedures such as layering with hexanes, diffusion of hexanes vapors, or slow evaporation of the solvent are needed for successful crystal growth of (**1**–**4**)[$AlCl_4$].

The X-ray diffraction analysis of **1**[$AlCl_4$] shows the C_s-symmetric molecular structure for the cation (Figure 1). The C1–C2 bond between the corannulene moiety and the methyl group is an elongated single bond (1.578(5) Å). The average value of the C1-C2-C angles (109.4°) clearly indicates the sp^3 hybridization of the C2 atom. Alkylation of corannulene pulls this hub C atom away from the surface with a

[*] Dr. A. V. Zabula, S. N. Spisak, Dr. A. S. Filatov, Prof. Dr. M. A. Petrukhina
Department of Chemistry, University at Albany
State University of New York
Albany, NY 12222 (USA)
Fax: (+1) 518-442-3462
E-mail: marina@albany.edu
Dr. A. Y. Rogachev
Institute für Anorganische und Angewandte Chemie
Universität Hamburg, 20146 Hamburg (Germany)

[**] Financial support of this work from the National Science Foundation Career Award (CHE-0546945) is gratefully acknowledged. We also thank Prof. L. T. Scott (Boston College) for fruitful discussions.

Supporting information for this article is available on the WWW under http://dx.doi.org/10.1002/anie.201007762.

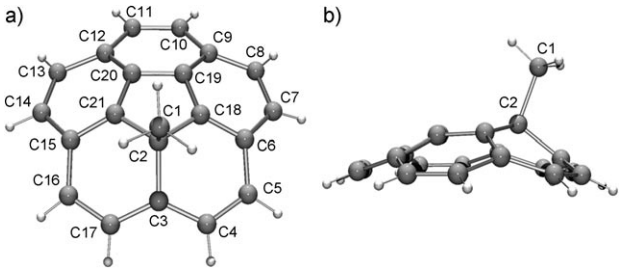

Figure 1. Molecular structure of **1**: a) top and b) side views.

Table 1: Selected distances [Å] and angles [°] for **1**–**4**.

	1	2	3	4
C1–C2	1.578(5)	1.577(5)	1.581(3)	1.613(7)
C2–C3	1.487(5)	1.503(4)	1.488(3)	1.499(7)
C2–C_{hub}[a]	1.477(5)	1.497(4)	1.496(3)	1.505(7)
C1–Cl	–	1.791(3)	1.771(2)[a]	1.766(5)[a]
C2···X[b]	0.49	0.50	0.50	0.51
C3···X[b]	0.02	0.02	0.04	0.03
C1-C2-C[a]	109.4	109.7	109.5	110.0

[a] Average values. [b] Distance between the C atom and the plane passing through the three neighboring atoms.

resulting shift of 0.29 Å. The C2–C18 and C2–C21 bond lengths (1.469(5) and 1.484(5) Å) are significantly longer than the conjugated C–C hub bonds in the parent corannulene (average 1.414(2) Å).[9] In turn, the two adjacent hub bonds (C18–C19 and C20–C21) become significantly shorter (1.368(5) Å), while the C19–C20 bond length remains essentially unchanged compared to that in $C_{20}H_{10}$ (1.410(5) Å). Thus, the central five-membered ring exhibits a more diene-like structure than that of corannulene. The C2–C3 spoke bond is most strongly affected by methylation (1.487(5) vs. 1.378(2) Å in $C_{20}H_{10}$), while all the other spoke bond lengths are only slightly elongated (averaged at 1.388(5) Å). Interestingly, three rim C–C bonds remain the same (average values of 1.381(6) vs. 1.380(2) Å in $C_{20}H_{10}$), while the C7–C8 and C13–C14 bonds become considerably shortened (1.350(5) Å). The peculiar bond length variation in **1** is related to the charge redistribution on the corannulene surface upon cation formation. Atoms C7, C8, C13, and C14 become the most negatively charged (as well as C4 and C17), and C3, C18, and C21 bear the most positive charge (see Table S3). In general, the geometric parameters of cations **2**–**4** follow similar trends as those in **1** (Figure 2, Table 1).

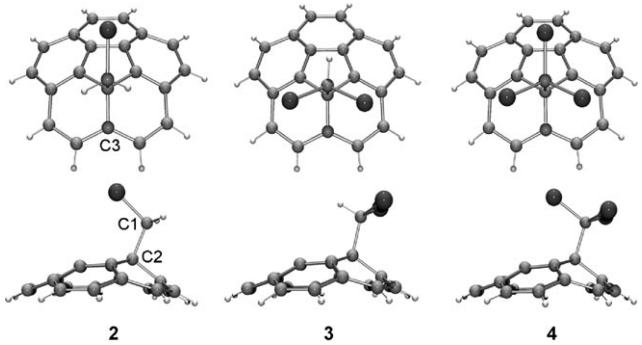

Figure 2. Molecular structures of **2**–**4**.

In the solid state, cations **1**–**4** exhibit different aggregation behavior, depending on the steric volume of the attached R group (Figure 3). Cations **1** assemble into 1D infinite columns based on strong concave–convex π–π stacking interactions (ca. 3.5–3.7 Å) that result from the complementarity of their electrostatic potential surfaces. Such packing is not found in the crystal structure of the parent corannulene,[9] but is generally observed in polyarenes with deeper bowls.[10] Cation

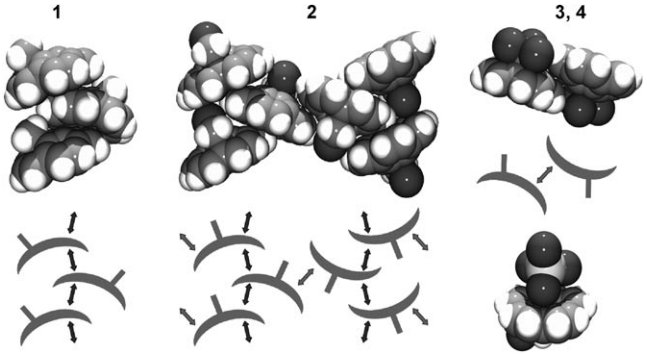

Figure 3. π–π stacking of cations **1**–**4** in crystals. Insertion of the $[AlCl_4]^-$ ion into the π bowl of corannulene in **3** (bottom right).

2 is linked by similar but weaker π–π interactions. The resulting 1D stacks are additionally connected by π–π convex–convex interactions (ca. 3.5–3.8 Å) into a 2D network. Further expansion of the R-group volume gives only bimolecular aggregates of corannulene cations **3** and **4**, which are held together by weak π–π convex–convex interactions.

Interestingly, the concave surfaces of **3** and **4**, which do not participate in π–π interactions, engage in electrostatic interactions with the $[AlCl_4]^-$ counterions to form extended 1D binary stacks in the former and a 2D layered structure in the latter product. In both solids, the $[AlCl_4]^-$ ion interacts with the concave surface of corannulene cations; these compounds represent the first reported examples where an anionic species is placed into a π bowl (Figure 3).[11] The Cl atom of $[AlCl_4]^-$ sits inside the cationic bowl, and the distances to the center of the five-membered ring of $C_{20}H_{10}$ are 3.566(2) and 3.315(5) Å in **3** and **4**, respectively.

Crystals of (**1**–**4**)$[AlCl_4]$ can be redissolved in CD_2Cl_2 or $CDCl_3$ to allow full characterization of the species in solution. The ^1H NMR spectra of cations **1**–**3** demonstrate the significantly high-field-shifted resonance signals for the CH_xCl_{3-x} groups (0.12 ppm, 2.08 ppm, and 4.01 ppm for **1**, **2**, and **3**, respectively) compared to those of CH_3CH_3 ($\delta = 0.85$ ppm), CH_3CH_2Cl ($\delta = 3.51$ ppm), and CH_3CHCl_2 ($\delta = 5.90$ ppm). This observation shows a strong shielding of the CH_xCl_{3-x} group from the aromatic 18-π-electron system. The resonance signals of the aromatic protons in cations **1**–**4** appear as four doublets ($^2J_{HH} \approx 8.7$ Hz) and one singlet signal in the range $\delta = 8.5$–9.3 ppm.

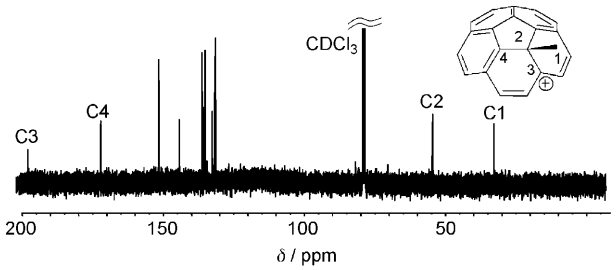

Figure 4. ^{13}C NMR spectrum of **1**.

The ^{13}C NMR spectra of **1**–**4** contain twelve signals, thus also confirming the C_s symmetry of the bowl-shaped carbocations (Figure 4). The signal of the cationic C3 center in **1** appears at 196 ppm. The position of this signal in **2**–**4** ranges from 191 to 187 ppm (Table 2). These values compare well

Table 2: Key ^{13}C chemical shifts [ppm] for **1**–**4**.

	1	2	3	4
C3	196	191	188	187
C4	170	167	166	167
C2	53	55	59	–[a]
C1	31	52	73	–[a]

[a] Not observed because of low solubility and decomposition.

with those found in the ^{13}C NMR spectra of C_{70}–$CHCl_2^+$ (198 ppm, in CF_3SO_3H)[6b] and in the protonated form of C_{60} (182 ppm, 1,2-$C_6H_4Cl_2$).[12] The slight high-field shifts of the C3 resonances of the chlorinated cations **2**–**4** compared to that of **1** can most probably be attributed to the interaction of unshared electron pairs at the Cl atoms of the R groups with the cationic C3 center. Similar interactions were postulated for the C_{60}–$CHCl_2^+$ and C_{60}–$CCl_2CH_2Cl^+$ ions.[6]

The chemical shifts of C4 (166–170 ppm) in **1**–**4** indicate a significant amount of positive charge at this carbon atom. The signal for C2 (53–59 ppm) is typical for aliphatic carbon atoms. Importantly, this signal demonstrates the exclusion of C2 from the aromatic system of the corannulene core, thus also indicating the sp^3 hybridization of this atom. For comparison, the corresponding C–H resonance signal of the $C_{60}H^+$ cation is detected at 56 ppm.[12] The chemical shift of the methyl group in **1** at 31 ppm shows the absence of a significant positive charge on the Cl atom, thus implying its strong delocalization over the curved polyaromatic surface. The substitution of hydrogen atoms of the CH_3 group in **1** by chlorine atoms leads to downfield shifts (by ca. 21 ppm) of the C1 resonance in **2** and **3** (Table 2).

The UV/Vis spectra of cations **1**–**4** measured in chloroform show a strong dependence of the absorption maximum of the π–π* transition band on the CH_xCl_{3-x} substituent (Figure 5). Whilst the corresponding maximum for the solution of **1** is detected at 560 nm, each subsequent substitution of a hydrogen atom of the CH_3 moiety by a chlorine atom leads to a bathochromic shift of approximately 23 nm.

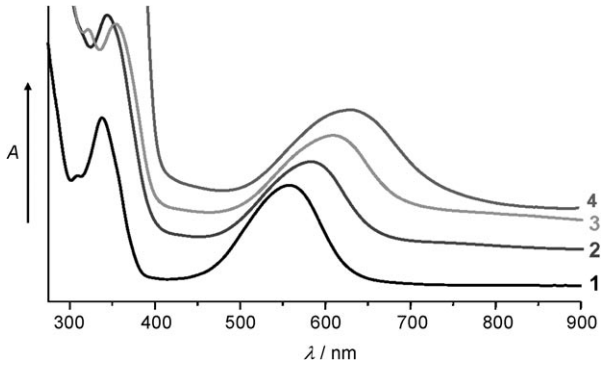

Figure 5. UV/Vis spectra for the cations **1**–**4** ($CDCl_3$).

The transfer of positive charge from R^+ to the corannulene core can be best illustrated by the change of the molecular electrostatic potential surface in $C_{20}H_{10}CH_3^+$ (Figure 6).[8] The delocalization of the charge provides a

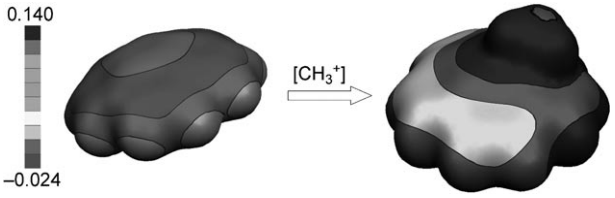

Figure 6. Molecular electrostatic potential surfaces for $C_{20}H_{10}$ and $C_{20}H_{10}CH_3^+$ (**1**).

remarkable thermodynamic stability for these cationic species. In contrast to planar polyaromatic systems, electrophilic attack of the R^+ group at a hub C atom of corannulene also alleviates the pyramidalization strain at that atom. The total energetic effect is large enough to fully trap the reactive $CH_xCl_{3-x}^+$ species at the hub site. The excellent delocalization ability of the nonplanar surface of corannulene was also recently demonstrated for radicals.[13]

In conclusion, site-specific alkylation of the curved corannulene surface under Friedel–Crafts reaction conditions resulted in bowl-shaped arenium carbocations, which were isolated as pure bulk crystalline solids with $[AlCl_4]^-$ counterions. The first X-ray diffraction analysis of these products revealed the perturbation of bowl-shaped structures caused by the interior surface functionalization. This work significantly expands the rare examples of any sort of reactivity at the interior carbon atoms of polyaromatic hydrocarbons.[14] It should also open practical routes for utilizing C–C covalent-bond-forming reactions for target derivatization of π-bowl surfaces. Moreover, this work illustrates that the strain energy stored within the curved nonplanar structures can be used to trap reactive intermediates, such as a CH_3^+ cation. We can anticipate the potential application of these reactions as a useful tool for the structural characterization of a variety of elusive chemical species.

Received: December 9, 2011
Published online: February 17, 2011

Keywords: carbocations · corannulenes · density functional calculations · electrophilic addition · structure elucidation

[1] For reviews, see: a) P. W. Rabideau, A. Sygula, *Acc. Chem. Res.* **1996**, *29*, 235 – 242; b) V. M. Tsefrikas, L. T. Scott, *Chem. Rev.* **2006**, *106*, 4868 – 4884; c) Y.-T. Wu, J. S. Siegel, *Chem. Rev.* **2006**, *106*, 4843 – 4867; d) A. S. Filatov, M. A. Petrukhina, *Coord. Chem. Rev.* **2010**, *254*, 2234 – 2246.

[2] a) T. J. Seiders, E. L. Elliott, G. H. Grube, J. S. Siegel, *J. Am. Chem. Soc.* **1999**, *121*, 7804 – 7813; b) G. Xu, A. Sygula, Z. Marcinow, P. W. Rabideau, *Tetrahedron Lett.* **2000**, *41*, 9931 – 9934; c) H. B. Lee, P. R. Sharp, *Organometallics* **2005**, *24*, 4875 – 4877; d) T. Amaya, T. Nakata, T. Hirao, *J. Am. Chem. Soc.* **2009**, *131*, 10810 – 10811; e) R. Maag, B. H. Northrop, A. Butterfield, A. Linden, O. Zerbe, Y. M. Lee, K.-W. Chi, P. J. Stang, J. S. Siegel, *Org. Biomol. Chem.* **2009**, *7*, 4881 – 4885; f) B. D. Steinberg, E. A. Jackson, A. S. Filatov, A. Wakamiya, M. A. Petrukhina, L. T. Scott, *J. Am. Chem. Soc.* **2009**, *131*, 10537 – 10545.

[3] A. Yu. Rogachev, M. A. Petrukhina, *J. Phys. Chem. A* **2009**, *113*, 5743 – 5753.

[4] D. V. Preda, L. T. Scott, *Tetrahedron Lett.* **2000**, *41*, 9633 – 9637.

[5] L. T. Scott, H. E. Bronstein, D. V. Preda, R. B. M. Ansems, M. S. Bratcher, S. Hagen, *Pure Appl. Chem.* **1999**, *71*, 209 – 219.

[6] a) T. Kitagawa, H. Sakamoto, K. Takeuchi, *J. Am. Chem. Soc.* **1999**, *121*, 4298 – 4299; b) T. Kitagawa, Y. Lee, N. Masaoka, K. Komatsu, *Angew. Chem.* **2005**, *117*, 1422 – 1425; *Angew. Chem. Int. Ed.* **2005**, *44*, 1398 – 1401.

[7] M. Riccò, D. Pontiroli, M. Mazzani, F. Gianferrari, M. Pagliari, A. Goffredi, M. Brunelli, G. Zandomeneghi, B. H. Meier, T. Shiroka, *J. Am. Chem. Soc.* **2010**, *132*, 2064 – 2068.

[8] See the Supporting Information for detailed synthetic procedures, characterization, X-ray diffraction study, and DFT calculations.

[9] a) J. C. Hanson, C. E. Nordman, *Acta Crystallogr. Sect. B* **1976**, *32*, 1147 – 1153; b) M. A. Petrukhina, K. W. Andreini, J. Mack, L. T. Scott, *J. Org. Chem.* **2005**, *70*, 5713 – 5716.

[10] A. S. Filatov, L. T. Scott, M. A. Petrukhina, *Cryst. Growth Des.* **2010**, *10*, 4607 – 4621.

[11] a) T. Amaya, H. Sakane, T. Hirao, *Angew. Chem.* **2007**, *119*, 8528 – 8531; *Angew. Chem. Int. Ed.* **2007**, *46*, 8376 – 8379; b) B. L. Schottel, H. T. Chifotides, K. R. Dunbar, *Chem. Soc. Rev.* **2008**, *37*, 68 – 83.

[12] a) C. A. Reed, K.-C. Kim, R. D. Bolskar, L. J. Mueller, *Science* **2000**, *289*, 101 – 104; b) L. J. Mueller, D. W. Elliott, G. M. Leskowitz, J. Struppe, R. A. Olsen, K.-C. Kim, C. A. Reed, *J. Magn. Reson.* **2004**, *168*, 327 – 335.

[13] A. Ueda, S. Nishida, K. Fukui, T. Ise, D. Shiomi, K. Sato, T. Takui, K. Nakasuji, Y. Morita, *Angew. Chem.* **2010**, *122*, 1722 – 1726; *Angew. Chem. Int. Ed.* **2010**, *49*, 1678 – 1682.

[14] a) H. E. Bronstein, L. T. Scott, *J. Org. Chem.* **2008**, *73*, 88 – 93; b) A. S. Filatov, A. Yu. Rogachev, E. A. Jackson, L. T. Scott, M. A. Petrukhina, *Organometallics* **2010**, *29*, 1231 – 1237.

